

High-Pressure Studies of Rotational Dynamics for Coumarin 153 in Alcohols and Alkanes

Naoki Ito and Okitsugu Kajimoto

Graduate School of Science, Kyoto University, Sakyo-ku, Kyoto 606-8502, Japan

Kimihiko Hara*

Research Center for Low Temperature and Materials Sciences, Kyoto University, Sakyo-ku, Kyoto 606-8502, Japan

Received: January 23, 2002

Subpicosecond fluorescence anisotropy measurements are used to characterize the rotational dynamics of coumarin 153 (C153) at high pressures in a series of alcohol and alkane solvents. Rotational correlation times (τ_R) are determined as a function of solvent viscosity to reveal the effect of the frictional behavior of the solvent. The results of the viscosity dependence of τ_R were compared with those predicted by the hydrodynamic model. Bimodal anisotropy decays of excited C153 are observed only in alcohol solvents. The specific viscosity dependence of τ_R in alcohols, which is observed when the solvent viscosity is varied by changing the pressure, is discussed on the basis of the pressure dependence on the solute–solvent and solvent–solvent interactions in alcohols.

I. Introduction

Understanding the molecular motion of rotational reorientation in solution provides direct information about the frictional coupling between a solute molecule and its solvent surroundings. For this reason, the study of the rotational reorientation dynamics in solution has long been a subject of interest in physical chemistry.¹

Molecular motion in a dense liquid should be influenced by both microscopic and hydrodynamic (or collective) effects. The earliest theoretical approaches to describe the friction due to rotational reorientation in solution are simple hydrodynamic theories, such as the Stokes–Einstein–Debye (SED) model,^{2,3} which is the foundation of many theoretical descriptions. The SED model assumes that the solvent is a structureless continuum and that the molecular details of solute–solvent interactions are neglected. As a consequence, those simple hydrodynamic models break down for the molecular motion of relatively small solute molecules, the motion in a solvent such as alcohol having specific interactions, and the motion with sufficiently short time scales. Recent interest in rotational dynamics has mainly focused on studying the deviations from simple hydrodynamic predictions in an effort to understand what they might reveal about the microscopic aspects of solvent friction.

To change the solvent friction, most of the previous studies have been performed by changing the solvents.^{4–7} In this method, the solute–solvent interaction and the solute/solvent size ratio are changed simultaneously. In some cases,^{8–12} the viscosity has been varied by changing the temperature. For the present purpose, varying the pressure can be used as a favorable method of changing the solvent viscosity,^{13–15} since it enables us to change the solvent viscosity in a single solvent widely and continuously without serious modification of the solvent-shell structure and with keeping a constant solute/solvent size ratio. Through this experimental approach, an isoviscous condi-

tion can be produced among different solvents. The differences in rotational correlation times among isoviscous fluids may reveal the effect of microscopic features such as hydrodynamic volume and solute–solvent and solvent–solvent interactions on rotational reorientation dynamics.

In this study we measured time-dependent fluorescence anisotropy of a dipolar solute, coumarin 153 (C153), at high pressures in a series of *n*-alcohol and *n*-alkane solvents. The rigid dye molecule, C153, was chosen mainly because it is a well-studied molecule at atmospheric pressure due to the large dipole-moment jump upon excitation, which may indicate a large interaction with polar solvents.^{16,17} Especially the rotational correlation times in a series of *n*-alcohol solvents were studied as a function of solvent shear viscosity. Many previous studies were concerned with aprotic and nonpolar solvents. In this paper the role of microscopic contribution and its pressure effect in alcohols are discussed compared with those of nonpolar *n*-alkane solvents. The results are also compared with our previous ones of the much less polar solute *p*-terphenyl (PTP), whose shape is assumed as a prolate symmetric top.¹⁵

II. Experimental Section

Laser grade C153 (Lambda Physik) was used as received. Solvents were obtained from Nakarai Tesque with highest purity, except that *n*-decane was from Aldrich. The concentrations of the solutions were $\sim 5 \times 10^{-5}$ M. All spectroscopic measurements were performed at 297 ± 0.5 K.

Time-resolved fluorescence anisotropies were measured at high pressures using femtosecond up-conversion techniques, which are practically based on the design of Maroncelli and co-workers,¹⁶ as shown in Figure 1. The excitation light source is a Ti:sapphire laser (Spectra-Physics, Tsunami model 3960) pumped by a Nd:YVO₄ diode laser (Millennia V). This laser system provides output pulses of 80 fs duration over a wavelength range of 790–800 nm and a repetition rate of 80 MHz. The second harmonic of the fundamental is generated

* To whom correspondence should be addressed. E-mail: hara@kuchem.kyoto-u.ac.jp. Fax: +81 75 753 3975.

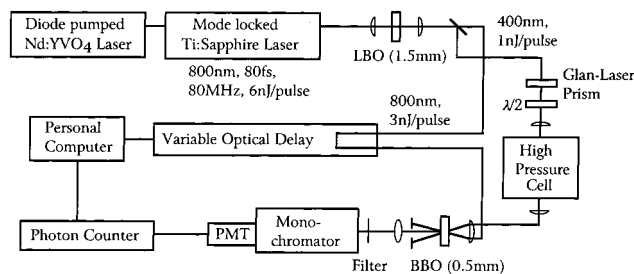


Figure 1. Schematic diagram of the fluorescence up-conversion laser system used for high-pressure measurements. The details are described in the text.

by type I mixing in a 1.5 mm LBO crystal having an energy of 1 nJ/pulse. Doubled pulses are separated from the fundamental with a dichroic beam splitter. The fluorescence signal from the sample solution is focused into a 0.5 mm BBO crystal with a 50 mm focal lens. The residual fundamental beam vertically polarized is subjected to a variable optical delay and focused into the same BBO crystal with the same lens, which serves as the gate pulse for up-converting the sample emission. The up-converted light is filtered, monochromatized by a monochromator (Oriel, model 77200), and detected with a photomultiplier. The excitation wavelength (λ_{exc}) is 400 nm. The overall instrumental response of this system is typically ~ 500 fs (fwhm), as judged by the cross-correlation between the pump and gate pulses.

Polarization of the excitation beam to the gate beam was controlled by a Glan-laser prism and a half-wave plate before the sample cell. For anisotropy measurements, a half-wave plate was rotated between the vertical and 45° positions to measure parallel ($I_{\parallel}(t)$) and perpendicular ($I_{\perp}(t)$) signals.

The high-pressure optical cell and pressure-generating system utilized for the present measurements have been described in detail elsewhere.¹⁸ Pressure-induced polarization scrambling by optical windows may render uncertainty to the measurement of the fluorescence polarization at high pressures. In this work fused quartz was used as the window material to avoid the pressure-induced polarization scrambling. Thereby, the maximum pressure was limited to 200 MPa. As reported by Crysomallis et al.,¹⁹ its correction in fused quartz within this pressure range is comparatively small and negligible. This fact is also confirmed by the initial anisotropy ($r(t=0)$) as described below.

The time-dependent fluorescence anisotropy excited by linearly polarized light is defined as

$$r(t) = \frac{I_{\parallel}(t) - I_{\perp}(t)}{I_{\parallel}(t) + 2I_{\perp}(t) - 3b} \quad (1)$$

where $I_{\parallel}(t)$ and $I_{\perp}(t)$ denote the fluorescence intensities of parallel-polarized and perpendicular-polarized components with respect to the polarization of the exciting beam, respectively. The background contribution (b) was determined by the signal level at $t < 0$. The difference in sensitivity between the two polarizations was confirmed as negligibly small by means of the tail matching of up-converted signals at longer time scales. The time-resolved fluorescence anisotropy ($r(t)$) was directly calculated from the parallel and perpendicular decay curves without deconvolution, since the rotational time scale observed here is much longer than the instrumental response.

III. Results

Figure 2 shows the typical decay curves for the vertically (parallel) and horizontally (perpendicular) polarized components

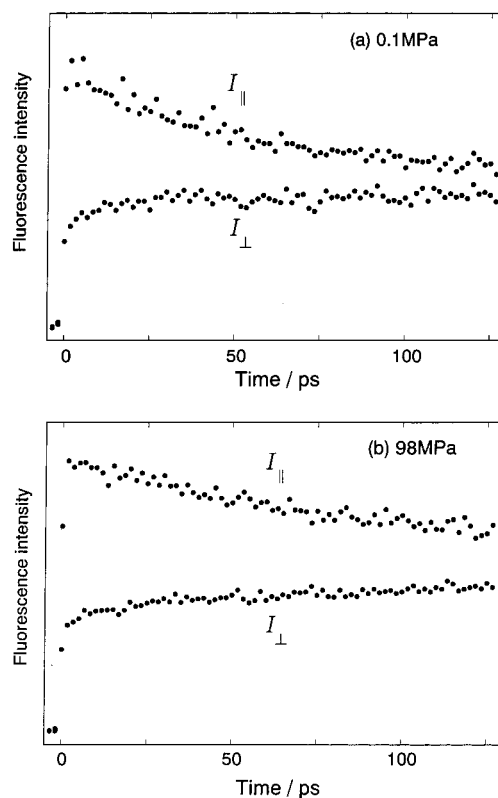


Figure 2. Representative parallel ($I_{\parallel}(t)$) and perpendicular ($I_{\perp}(t)$) components of the fluorescence decays of excited C153 in ethanol ($\lambda_{\text{exc}} = 400$ nm) at (a) 0.1 MPa and (b) 98 MPa.

of the fluorescence of C153 in ethanol at atmospheric pressure ($=0.1$ MPa) and 98 MPa. The anisotropy $r(t)$ was constructed from both intensities $I_{\parallel}(t)$ and $I_{\perp}(t)$ according to eq 1. The anisotropy decays corresponding to Figure 2 are shown in Figure 3. By using a nonlinear least-squares algorithm, the anisotropy data were fitted to monoexponential or biexponential functions of times as follows:

$$r(t) = r(0)\{a_1 \exp(-t/\tau_1) + a_2 \exp(-t/\tau_2)\} \quad (2)$$

where $a_1 + a_2 = 1$. The fits were achieved by simultaneously varying all four parameters, i.e., $r(0)$, a_1 , τ_1 , and τ_2 . Results of such fits are provided in Figure 3 for ethanol at 0.1 and 98 MPa. The two time values of τ_1 and τ_2 thus obtained for electronically excited C153 are presented in Table 1 together with the initial anisotropy ($r(0)$) and the amplitude of the slow component ($a_2 (=1 - a_1)$). Also listed are the average rotational correlation times ($\langle\tau_R\rangle$):

$$\langle\tau_R\rangle = a_1\tau_1 + a_2\tau_2 \quad (3)$$

We find that the resulting $r(0)$ values lie within the range 0.34–0.39 irrespective of the solvents as well as pressures. This agrees well with the result by Horng et al.,¹⁷ although it is slightly lower than the theoretical limiting value for the parallel dipoles between absorption and emission. Note that the invariable value of $r(0)$ against pressure demonstrates that the pressure effect on window birefringence of the high-pressure cell is negligible.

The following results can be deduced. In the case of alcohol solvents, the fluorescence anisotropy decays of dipolar C153 are well represented by a biexponential function of time, while in alkane solvents the anisotropy decay is adequately described by a monoexponential function ($a_1 = 1$). In the case of nonpolar PTP solute, on the other hand, the anisotropy decays in both

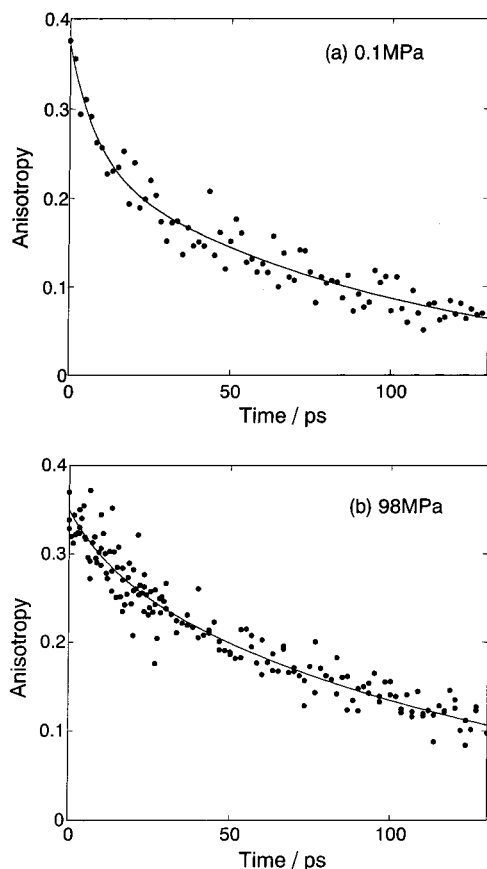


Figure 3. Representative fluorescence anisotropy decays $r(t)$ of C153 in ethanol fitted by a biexponential function at (a) 0.1 MPa and (b) 98 MPa. The solid lines through the data points represent the biexponential fit to the $r(t)$ data.

alcohol and alkane solvents are completely represented by monoexponential functions. The nonexponential anisotropy decay has often been attributed to nonexponential anisotropy motions which are caused by different friction constants for the rotation about different molecular axes. However, this contribution is ruled out for the present case of alcohols, because the nonexponential behavior does not appear in alkane solvents at all, even at the highest viscosity condition. Namely, if there is a corresponding fast component, we could observe it for *n*-decane at 192 MPa, since the present time resolution is high enough. Furthermore, in the case of aprotic polar solvents such as acetonitrile and acetone, the anisotropy decays are well represented by a monoexponential function.

As an alternative explanation, in the case of alcohols, a large contribution of dielectric friction will be expected. It has been reported, however, that the basic notion of the dielectric friction is not appropriate.¹⁷ As a consequence, we come to the conclusion that the nonexponential anisotropy decay in alcohol is caused by the effect of specific solute–solvent interaction owing to the character of hydrogen-bonding formation for excited C153 with alcohols.

The present time values of C153 in *n*-alcohols at atmospheric pressure are in good agreement with previous results,¹⁷ although the temperature at which they are measured is slightly different. Figure 4 shows a plot of $\langle\tau_R\rangle$ values from Table 1 as a function of solvent viscosity (η). The solvent viscosity data at high pressures were obtained from the literature.^{20–23} The most striking feature of Figure 4 is that $\langle\tau_R\rangle$ values of alcohol solvents follow a different viscosity correlation as compared with those of alkane solvents. This means that C153 rotates considerably

TABLE 1: Solvent Viscosity and Rotational Anisotropy Decay Parameters of C153 at High Pressures

pressure (MPa)	η (mPa s)	τ_1 (ps)	τ_2 (ps)	a_2	$\langle\tau_R\rangle$ (ps)	C_{obs}	$r(0)$
Methanol							
0.1	0.56	3	45	0.77	35 (35) ^a	0.62	0.37
118	0.87	4	58	0.85	50	0.58	0.37
177	1.0	1	67	0.91	61	0.61	0.34
Ethanol							
0.1	1.1	8.5	99	0.64	66 (63) ^a	0.60	0.37
50	1.4	11	108	0.79	88	0.63	0.35
98	1.7	14	130	0.83	110	0.65	0.35
1-Propanol							
0.1	2.1	6	178	0.70	126 (101) ^a	0.60	0.35
49	2.9	15	240	0.74	180	0.62	0.36
98	4.0	16	269	0.78	213	0.53	0.37
147	5.3	11	339	0.82	280	0.53	0.36
196	7.0	28	440	0.85	378	0.54	0.36
1-Butanol							
0.1	2.6	10	220	0.70	157 (140) ^a	0.61	0.38
98	5.1	16	351	0.77	274	0.54	0.38
147	6.5	5	382	0.89	341	0.53	0.38
<i>n</i> -Octane							
0.1	0.52	22			22	0.42	0.38
98	1.2	36			36	0.30	0.35
147	1.6	63			63	0.39	0.37
196	2.1	70			70	0.33	0.39
<i>n</i> -Decane							
0.1	0.87	28			28	0.32	0.36
98	2.2	77			77	0.35	0.35
147	3.2	106			106	0.33	0.36
192	4.4	147			147	0.33	0.36

^a From ref 17.

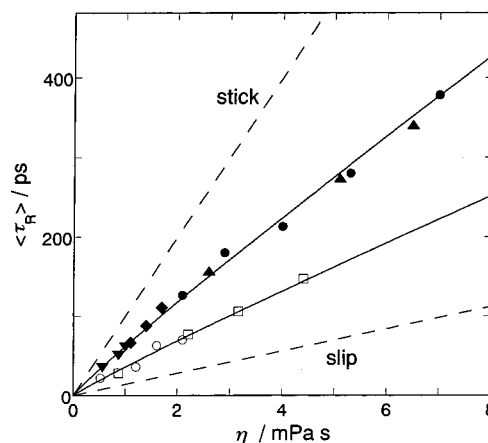


Figure 4. Averaged rotational correlation time $\langle\tau_R\rangle$ of C153 as a function of solvent viscosity η in methanol (\blacktriangledown), ethanol (\blacklozenge), 1-propanol (\bullet), 1-butanol (\blacktriangle), *n*-octane (\circ), and *n*-decane (\square). Dashed lines represent the rotation times predicted from hydrodynamic calculations assuming slip and stick boundary conditions for an ellipsoidally shaped solute.

slower in alcohol solvents than in alkane solvents for identical viscosity. We find that both solvent classes exhibit nearly proportional correlation against viscosity. The rotation times with viscosity are expressed by a power-law relation, $\langle\tau_R\rangle \propto \eta^\alpha$; the parameter α is 0.93 for alcohols and 0.94 for alkanes. Note that both are close to unity and there is no significant difference between them.

IV. Discussion

Many hydrodynamic theories describing the motion of rotational reorientation in liquids have started from the SED

model,^{2,3} which predicts a constant value of τ_R/η . It is mostly the case that the SED model assuming a spherical solute and continuum solvent is too simple to describe real molecular systems. Understanding the deviation of experimental results from the simple SED prediction, however, provides an insight into *molecular* aspects in solution. The primary candidate for the reason for this deviation is the breakdown of the prerequisite in the SED model, that is, a “spherically shaped solute” and “continuum solvent” in which the solvent size is assumed as small enough compared with the solute size.

An alternative cause of the deviation from the hydrodynamic approaches, which has not been considered in detail so far, is the different solute–solvent and solvent–solvent interactions. The solvent viscosity, which is used as a scaling factor, includes the contribution of solvent–solvent interactions, but it does not include the contribution of solute–solvent interactions at all. In the case where the solute–solvent interaction is weaker than the solvent–solvent interaction, τ_R should deviate toward a smaller value than predicted by the SED approach.

A. Deviation from the Hydrodynamic Model. According to the modified SED equations given by Perrin²⁴ and Kivelson et al.,²⁵ in which the effects of shape and size for both solute and solvent molecules are taken into account, the rotational correlation time τ_R has been described by the following functional form:

$$\tau_R = \frac{V\eta}{k_B T} fC + \tau_0 \quad (4)$$

where V is the hydrodynamic volume of the rotating solute molecule, f is a parameter ($f \geq 1$) which is dependent on the molecular shape of the solute, C is a parameter which is dependent on hydrodynamic boundary conditions ($C = 1$ for the “stick” condition and $C < 1$ for the “slip” condition²⁶), τ_0 is the free rotor relaxation time related to the moment of inertia,²⁷ k_B is the Boltzmann constant, and T is the temperature. In the case of both parameters f and C being equal to unity, eq 4 reduces to the original simple SED equation. From the linear fitting, the small positive intercept at zero viscosity corresponds to τ_0 , which falls around 10 ps for both solvents. This may be considered as reflecting the inertial contribution in τ_R , but it is hard to discuss this point further in detail until the more accurate measurement at lower viscosity is performed.

Under stick boundary conditions, one envisages that a solvent layer sticks to the solute surface and moves in union with the solute surface. An alternative extreme is slip boundary conditions, in which the torque on the rotating molecule is determined by the force required to displace the surrounding molecule as the solute rotates. In general, stick boundary conditions describe the rotational reorientation of large molecules in solution. Slip boundary conditions provide a description for the motion of small molecules. The results of hydrodynamic calculations for stick and slip boundary conditions are also included in Figure 4. The calculations were performed as follows. The molecular shape of C153 can be reasonably approximated by an ellipsoid having axis dimensions $a = 0.4 \times 10^{-9}$ m, $b = 0.96 \times 10^{-9}$ m, and $c = 1.22 \times 10^{-9}$ m,¹⁷ and its volume is 2.46×10^{-28} m³ obtained from van der Waals increments.²⁸ For the case of PTP, the van der Waals volume is 2.3×10^{-28} m³, which was estimated by using the data by Bondi.²⁹ The dimension of the major axis of 1.6×10^{-9} m is estimated from the van der Waals radius. The dimension of the minor axis of 0.52×10^{-9} m is then determined by requiring the volume of the spheroid to be equal to the van der Waals volume of PTP, which is slightly

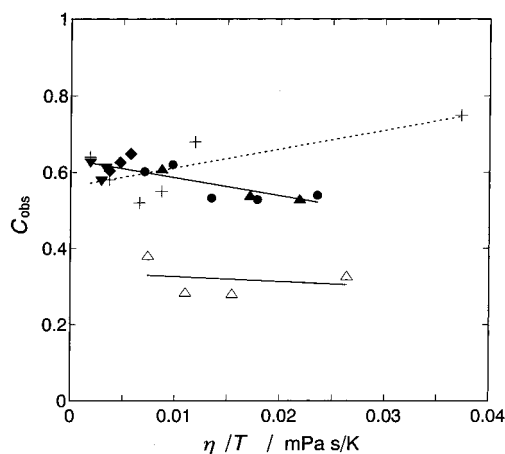


Figure 5. Comparison of C_{obs} of C153 and PTP in alcohols as a function of η/T : C153 in methanol (\blacktriangledown), ethanol (\blacklozenge), 1-propanol (\bullet), and 1-butanol (\blacktriangle) and PTP in 1-butanol (\triangle). Previous literature data (+)¹⁷ obtained by the solvent-changing method are included for comparison.

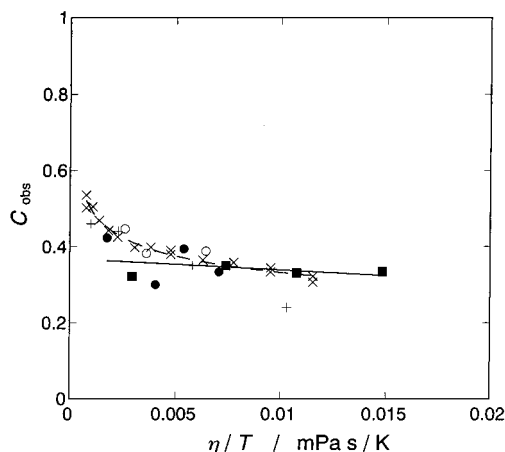


Figure 6. Comparison of C_{obs} of C153 and PTP in alkanes as a function of η/T : C153 in *n*-octane (\bullet) and *n*-decane (\blacksquare) and PTP in *n*-octane (\circ). Previous literature data (\times , +)^{6,17} obtained by the solvent-changing method are included for comparison.

smaller than the van der Waals radius of the phenyl ring.²⁹ As a result, we have $\rho = 3.07$. The f factors appropriate for both boundary conditions were calculated from Perrin’s equations.²⁴ The C value for stick boundary conditions is put equal to unity. The C value of C153 for slip boundary conditions is obtained by interpolating the numerical tabulation of the literature.^{30,31} For PTP it is from the paper by Hu and Zwanzig.²⁶

As seen in Figure 4, it is by an intermediate regime between the two extremes of stick and slip conditions that the present experimental results of C153 are indicated. However, the experimental $\langle\tau_R\rangle$ data of PTP fall appreciably lower than the slip extreme. This fact has been explained by the contribution of the free volume of the solvent.¹⁵

To examine the deviation from SED predictions further in detail, we plotted the observed C values (C_{obs}) of C153 and PTP against η in Figures 5 and 6. In these figures the previous data at atmospheric pressure are also represented for comparison. Note that C_{obs} can be equated to the ratio of $\langle\tau_R\rangle$ to the rotational time of stick conditions (τ_{stick}):

$$C_{\text{obs}} = \langle\tau_R\rangle/\tau_{\text{stick}} \quad (5)$$

The following observations and considerations can be deduced regarding the results represented in Figures 5 and 6.

(1) In the case of C153, there is a marked difference in $\langle\tau_R\rangle$ values between alcohol and alkane solvents. The $\langle\tau_R\rangle$ values of alcohol solvents lie closer to stick predictions, while those of alkanes are much faster than the stick line by roughly a factor of 3. However, $\langle\tau_R\rangle$ values of PTP in both solvents exhibit identical correlations with solvent viscosity. In previous papers,^{10,14,17} such behavior of alcohol solvents has been analyzed by the dielectric friction model. When the solvent dielectric constant of a solvent exceeds 10, the dielectric friction time (τ_{DF}), which has to be added to the rotation time, is related to the solute dipole moment (μ) and solvent dielectric constant (ϵ) according to the Nee–Zwanzig expression:³²

$$\tau_{DF} = \frac{\mu^2}{k_B T a^3} \frac{\epsilon - 1}{\epsilon_0 (2\epsilon + 1)^2} \tau_D \quad (6)$$

where a is the cavity radius, ϵ_0 is the permittivity of free space, and τ_D is the Debye relaxation time of the solvent. Performing the calculation of τ_{DF} values for the present data using eq 6, we found that the difference in $\langle\tau_R\rangle$ values between alcohol and alkane solvents cannot be explained by this model. For example, when we use the van der Waals radius, τ_{DF} in ethanol at 0.1 MPa obtained from eq 6 is 25 times larger than the present τ_R value. It should be noted, however, that when τ_{DF} is calculated by eq 6, the estimation of a and τ_D is a serious problem for quantitative discussion, since a spherical solute molecule and a single decay are assumed in the model.

Such specific behavior of alcohol solvents should originate from some additional stronger interaction of C153 with alcohols than alkanes. The stronger interaction may be expected from the excited C153 having a large dipole moment ($\mu(S_1) \approx 15$ D)³³ and capable of hydrogen-bonding with alcohols. This is also evidenced by the delocalized charge distribution in the excited state of C153, which has been evaluated from recent quantum chemical calculations.^{34,35}

(2) As for the case of C153 in alcohol solvents, a notable difference is observed for the rotational correlation times and their viscosity dependence between the two different experimental methods, i.e., when the viscosity is varied by changing the solvent and when it is varied by changing the pressure in methanol, ethanol, 1-propanol, and 1-butanol. Namely, when the viscosity is changed by changing the solvent, C_{obs} increases with η . When it is changed by changing the pressure, conversely C_{obs} decreases with η . The cause of this difference can be explained by the different strengths and their different pressure dependencies between solute–solvent and solvent–solvent interactions. The decreasing behavior of C_{obs} in the pressure-changing method is caused by the strengthening effect of solvent–solvent interactions with pressure. It should be noted that the strengthening of the hydrogen-bonding in alcohols with increasing pressure has been demonstrated by the measurements of NMR and Raman spectra at high pressures.^{36,37} However, in the solvent-changing method for a series of n -alcohols, the hydrogen-bonding character gradually decreases with increasing alkyl chain length of the n -alcohols, which has been determined from the measurement of the solvatochromic shift.³⁸ This fact leads to the increasing behavior of C_{obs} with η , as long as the solute–solvent interaction is relatively invariable among the series of alcohols.

Similar unexpected viscosity dependence with pressure has been reported by Philips et al.^{13,14} through the high-pressure study of anisotropy decay for an excited cationic solute, rhodamine 6G (R6G), in alcohols. They explained the behavior as based on the different changes in the solvent dielectric

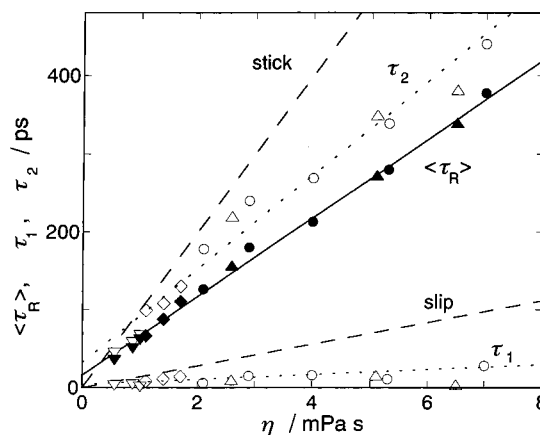


Figure 7. $\langle\tau_R\rangle$, τ_1 , and τ_2 of C153 in alcohols as a function of η : methanol (\blacktriangledown , \triangledown), ethanol (\blacklozenge , \lozenge), 1-propanol (\bullet , \circ), and 1-butanol (\blacktriangle , \triangle).

constant between the pressure-changing method and the solvent-changing method. Namely, the dielectric constant increases with increasing pressure, while it decreases with increasing chain length of the n -alcohols. The analogous reasoning might also be considered as possible for the present case. In the case of the dipolar solute C153, however, a much smaller effect of dielectric friction is expected, as compared with R6G having an ionic character.^{16,17} Therefore, more important than dielectric friction should be the specific hydrogen-bonding character in alcohols.

(3) As seen in Figure 6, for a series of nonpolar n -alkane solvents, C_{obs} becomes smaller with increasing molecular size of the solvent. This fact can be explained on the basis of the breakdown of the SED continuum assumptions. The larger the solvent volume with respect to the solute volume, the larger the deviation from the SED stick boundary predictions should become.

From Figures 5 and 6, we see that the C_{obs} values of PTP in 1-butanol and in n -octane seem coincident with each other, which is ~ 0.4 . On the basis of the solute–solvent size ratio, we may expect that the C_{obs} value of 1-butanol should fall around 0.6. We can conclude that the additional decrease will be caused by the weaker interactions between PTP and 1-butanol than between 1-butanol molecules.

B. Bimodal Behavior for Alcohol Solvents. Bimodal anisotropy decays of C153 are observed only in alcohol solvents, while those of nonpolar and polar aprotic solvents are completely described by monoexponential forms. Alcohol is characterized as an associative or hydrogen-bonding solvent. It would be natural to consider that this character leads to the bimodal anisotropy decay. The longer decay component would reflect the more collective contribution in solvent–solvent interactions against the rotational reorientation motion of the solute. In Figure 7, the two time values τ_1 and τ_2 of alcohols are plotted separately. The τ_2 values locate much closer to the line of stick boundary conditions, which reflects the collective motion of alcohols.

To discuss this behavior further on the basis of the present experimental results, the slow amplitude (a_2) is plotted as a function of η in Figure 8. For each alcohol a_2 increases with increasing η . Conversely, a_2 decreases with increasing chain length of the alcohols at isoviscosity conditions, although a large experimental deviation is included, especially for 1-butanol. This may also originate from the hydrogen-bonding character of alcohols. When the solvent–solvent interactions are strengthened with increasing pressure,^{36,37} the fraction of collective

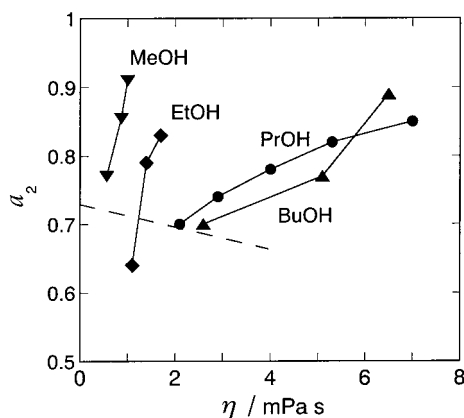


Figure 8. Slow amplitude a_2 of C153 in alcohols as a function of η . The dashed line represents the data at 0.1 MPa.

interaction in the alcohol should be increased. The fact that the hydrogen-bonding character of alcohols becomes weaker in the order of the chain length of n -alcohols³⁸ leads to the decreasing behavior of a_2 , as indicated by the dashed line in Figure 8.

V. Summary and Conclusions

To investigate the molecular motion of rotational reorientation in solution, we have measured in this work the fluorescence anisotropy decays of an excited dipolar solute (C153) and an excited nonpolar solute (PTP) at high pressures in a series of n -alcohol and n -alkane solvents. We utilized up-conversion laser techniques with a time resolution of 500 fs. High-pressure measurements were employed to change the solvent viscosity over a wide range. The primary objective of this work was to analyze the rotational dynamics of C153 to reveal the microscopic aspects of rotational dynamics in solution, especially in alcohols.

We observed unexpected results from this high-pressure study. The first is the observation that there is a marked difference in the rotational reorientational motion of C153 between alcohol and alkane solvents. Bimodal anisotropy decays are observed exclusively for n -alcohols. In addition, the τ_R values of alcohols locate closer to the stick boundary prediction of hydrodynamic theory as compared with those of alkane solvents. This difference is not caused by the contribution due to dielectric friction, but is caused by the greater solute–solvent interactions in alcohols compared with those in alkanes.

Second, the different viscosity dependencies of τ_R values between the pressure-changing method and the solvent-changing method are observed for alcohol solvents and not for alkane solvents. This can also be well explained on the basis of the hydrogen-bonding character of alcohols.

The third is the observation that the application of pressure leads to an increase in the collective contribution of rotational reorientational motion in alcohols.

We expect that further experiments at high pressures over the wider viscosity range will provide more insight into solution-phase chemistry.

Acknowledgment. We are grateful to Dr. A. Shimojima for his assistance in the laser instrumentation. This work was supported in part by a Grant-in-Aid for Scientific Research (No. 09640602) from the Ministry of Education, Science, Sports and Culture. Additional support was provided by Core Research for Evolutional Science and Technology (CREST) of the Japan Science and Technology Corp. (JST).

References and Notes

- (1) See for example: (a) *Rotational Dynamics of Small and Macromolecules*, 4th ed.; Dorfmueller, T., Pecora, R., Eds.; Springer-Verlag: Berlin, 1987; Vol. 293. (b) Fleming, G. R. *Chemical Applications of Ultrafast Spectroscopy*, Oxford: New York, 1986.
- (2) Einstein, A. *Ann. Phys. (Leipzig)* **1906**, *19*, 371.
- (3) Debye, P. *Polar Molecules*; Dover: New York, 1929.
- (4) Williams, A. M.; Jiang, Y.; Ben-Amotz, D. *Chem. Phys.* **1994**, *180*, 119.
- (5) Jiang, Y.; Blanchard, G. J. *J. Phys. Chem.* **1994**, *98*, 6436.
- (6) Benzler, J.; Luther, K. *Chem. Phys. Lett.* **1997**, *279*, 333.
- (7) Hartman, R. S.; Konitsky, W. M.; Waldeck, D. H.; Chang, Y. J.; Castner, E. W., Jr. *J. Chem. Phys.* **1997**, *106*, 7920.
- (8) Chuang, T. J.; Eiseenthal, K. B. *Chem. Phys. Lett.* **1971**, *11*, 368.
- (9) Anderton, R. M.; Kauffman, J. F. *J. Phys. Chem.* **1994**, *98*, 12117.
- (10) Wiemers, K.; Kauffman, J. F. *J. Phys. Chem. A* **2000**, *104*, 451.
- (11) Dutt, G. B.; Krishna, G. R. *J. Chem. Phys.* **2000**, *112*, 4676.
- (12) Dutt, G. B.; Krishna, G. R.; Raman, S. *J. Chem. Phys.* **2001**, *115*, 4732.
- (13) Philips, L. A.; Webb, S. P.; Yeh, S. W.; Clark, J. H. *J. Phys. Chem.* **1985**, *89*, 17.
- (14) Philips, L. A.; Webb, S. P.; Clark, J. H. *J. Chem. Phys.* **1985**, *83*, 5810.
- (15) Ito, N.; Kajimoto, O.; Hara, K. *Chem. Phys. Lett.* **2000**, *318*, 118.
- (16) Horng, M.-L.; Gardecki, J. A.; Papazyan, A.; Maroncelli, M. *J. Phys. Chem.* **1995**, *99*, 17311.
- (17) Horng, M.-L.; Gardecki, J. A.; Maroncelli, M. *J. Phys. Chem. A* **1997**, *101*, 1030.
- (18) Hara, K.; Morishima, I. *Rev. Sci. Instrum.* **1988**, *59*, 2397.
- (19) Chrysomallis, G. S.; Drickamer, H. G.; Weber, G. J. *Appl. Phys.* **1978**, *49*, 3084.
- (20) Bridgman, P. W. *Collected Experimental Papers*; Harvard University Press: Cambridge, MA, 1964; Vol. IV.
- (21) Brazier, D. W.; Freeman, G. R. *Can. J. Chem.* **1969**, *47*, 893.
- (22) Ducoulombier, D.; Zhou, H.; Boned, C.; Peyrelasse, J.; Saint-Guirons, H.; Xans, P. *J. Phys. Chem.* **1986**, *90*, 1692.
- (23) Stephan, K.; Lucas, K. *Viscosity of Dense Fluids*; Plenum Press: New York, 1979.
- (24) Perrin, F. *J. Phys. Radium* **1934**, *5*, 497.
- (25) Kivelson, D.; Kivelson, M. G.; Oppenheim, I. *J. Chem. Phys.* **1970**, *52*, 1810. Kivelson, D. *Discuss. Faraday Soc.* **1977**, *11*, 7.
- (26) Hu, C.-M.; Zwanzig, R. *J. Chem. Phys.* **1974**, *60*, 4354.
- (27) Bauer, D. R.; Brauman, J. R.; Pecora, R. *J. Am. Chem. Soc.* **1974**, *96*, 6840.
- (28) Edwards, J. T. *J. Chem. Educ.* **1970**, *47*, 261.
- (29) Bondi, A. *J. Phys. Chem.* **1964**, *68*, 441.
- (30) Youngren, G. K.; Acrivos, A. *J. Chem. Phys.* **1975**, *63*, 3846.
- (31) Senson, R. J.; Hochstrasser, R. M. *J. Chem. Phys.* **1993**, *98*, 2490.
- (32) Alavi, D. S.; Waldeck, D. H. *J. Chem. Phys.* **1991**, *94*, 6196; **1993**, *98*, 3580.
- (33) Baumann, W.; Nagy, Z. *Pure Appl. Chem.* **1993**, *65*, 1729.
- (34) Cichos, F.; Brown, R.; Bopp, P. A. *J. Chem. Phys.* **2001**, *114*, 6834.
- (35) Mühlpfordt, A.; Schanz, R.; Ernsting, N. P.; Farztdinov, V.; Grimme, S. *Phys. Chem. Chem. Phys.* **1999**, *1*, 3209.
- (36) Bai, S.; Yonker, C. R. *J. Phys. Chem. A* **1998**, *102*, 8641.
- (37) Shimizu, H.; Nakamichi, Y.; Sasaki, S. *J. Raman Spectrosc.* **1990**, *21*, 703.
- (38) Marcus, Y. *The Properties of Solvents*; John Wiley & Sons Ltd.: New York, 1998.